* Presently with Shell Pipeline Co., Houston, Texas.
[1] D. B. Spalding, J. Sci. Instrum. **27**, 310 (1950).
[2] R. Eichhorn and T. F. Irvine, Jr., Rev. Sci. Instrum. **29**, 33 (1958).
[3] K. Elgeti and E. R. G. Eckert, Chem. Ing. Tech. **37**, 1133 (1965).
[4] R. W. Swanson, Ph.D. thesis in Chem. Eng., University of Delaware, Newark, 1966.
[5] A. J. Karabelas, Ph.D. thesis in Chem. Eng., University of Illinois, Urbana, 1970.

THE REVIEW OF SCIENTIFIC INSTRUMENTS VOLUME 42, NUMBER 11 NOVEMBER 1971

Determination of Ion Transit Times in an Ion Cyclotron Resonance Spectrometer

T. B. McMahon and J. L. Beauchamp*
Arthur Amos Noyes Laboratory of Chemical Physics,† California Institute of Technology, Pasadena, California 91109
(Received 11 January 1971; and in final form, 7 May 1971)

A method for directly determining ion transit times in an ion cyclotron resonance spectrometer has been developed which employs a simple combination of pulsed ion formation and time dependent trapping conditions. The variation of transit times with the adjustable parameters associated with the experiment (magnetic field strength, drift voltage, trapping voltage, pressure, and ion kinetic energy) is examined and found to be in quantitative agreement with the predictions of electrodynamic theory. The accurate determination of ion transit times facilitates the calculation of ion–molecule reaction rate constants of increased credibility. In addition, a technique for recording single resonance spectra by trapping voltage modulation is presented.

INTRODUCTION

ION cyclotron resonance spectroscopy (ICR) is a relatively new mass spectrometric technique ideally suited for the study of ion–molecule reactions.[1] Using the techniques of double resonance[2,3] and ion ejection,[4–6] reaction sequences and product distributions may be determined. Pulse experiments have been developed which allow the variation of reaction rate constants with ion kinetic energy to be determined for very nearly monoenergetic ions in the energy range extending to 100 eV from thermal energies.[7,8] This leaves only the calculation of reaction rate constants at a particular ion energy (usually near thermal) to completely characterize the ion chemistry of a molecule. Equations to calculate ICR peak intensities from power absorption equations have been formulated and rate constants extracted from them both by approximate methods[9] and analysis involving iteration by computer.[9–11] Comprehensive equations for calculation of ICR line shapes, which include consideration of both reactive and nonreactive encounters, have been recently developed and applied to the determination of reaction probabilities and rate constants.[11]

In the more common experimental arrangement, ions are formed by electron impact in the source region of the ICR cell, drifted from the source to the resonance region, observed while drifting through the resonance region by a marginal oscillator–detector, and finally collected at the terminus of the resonance region to determine the total ion current. Two parameters pertinent to the above kinetic analysis are the time the ions enter the resonance region of the ICR cell, τ, and the time the ions leave the resonance region, τ'. The determination of rate constants depends on an accurate assessment of these quantities. Classical electrodynamic theory provides the analysis which has been used thus far to calculate simply these times from the magnetic field strength and voltages applied to the drift plates of the ICR cell.

The purpose of this paper is to present a new technique for experimentally measuring τ and τ' and determining the dispersion in transit times of ions from the electron beam to the total ion current monitor. Variation of ion transit times with various adjustable parameters is determined and discussed, including trapping voltage, drift voltage, magnetic field strength, pressure, and ion kinetic energy.

I. ANALYSIS OF ELECTROSTATIC FIELDS IN THE ICR CELL

Beauchamp and Armstrong[5] have presented an analysis of the electrostatic fields for ICR cells with equally spaced trapping and drift electrodes (square cell). Greater homogeneity for the drift field is attained by decreasing the spacing between the drift electrodes relative to the spacing between the trapping electrodes. In the present experiment, the standard Varian flat cell utilizing Vespel (Dupont) supports for the electrodes was employed. The spacing between trapping electrodes is 2.54 cm, twice the spacing between the drift electrodes. The distance between the electron beam and the resonance region is 2.54 cm; the length of the resonance region is 6.35 cm.

Equipotentials of the electrostatic fields in the cell have been determined both by applying appropriate voltages to silver electrodes painted on uniform resistance paper in accordance with the geometry of the flat cell and by an exact solution of Laplace's equation. With no applied drift voltages, a typical set of equipotentials arising from the trapping and drift voltages applied alone is illustrated in Fig. 1. In order to describe the effects of potentials applied to the drift and trapping electrodes on ion motion, it is

useful to parameterize the electrostatic fields in the cell. Following Beauchamp and Armstrong[5] the equipotentials shown in Fig. 1 which arise from the trapping voltage can be approximated by an asymmetric quadrupolar field of the general form

$$V=V_0+Az^2-Bx^2, \tag{1}$$

where V_0 is the potential at the center of the cell and the constants A and B are chosen to best match the boundary conditions. The origin of the coordinate system is taken at the center of the cell midway between the trapping and drift electrodes. A detailed solution to the electrostatic field equations gives $V_0 \cong 0.11 V_T$. If d is the spacing between the trapping plates, and Eq. (1) is to satisfy the boundary conditions at both $x=0, z=\pm d/2$ and $z=0, x=\pm d/4$, then $A \cong 3.52$, $B \cong 1.76$, and

$$V=V_T[0.11+(1.76/d^2)(2z^2-x^2)]. \tag{2}$$

The drift voltages are assumed to give rise to an idealized set of equipotentials appropriate to a parallel plate capacitor with

$$V=2xV_D/d, \tag{3}$$

where V_D is the drift voltage applied across the ICR cell. For reasons discussed in detail below, this voltage is nominally divided between the top and bottom plates of the cell. A set of equipotentials for typical experimental values of combined drift and trapping voltages is shown in Fig. 2.

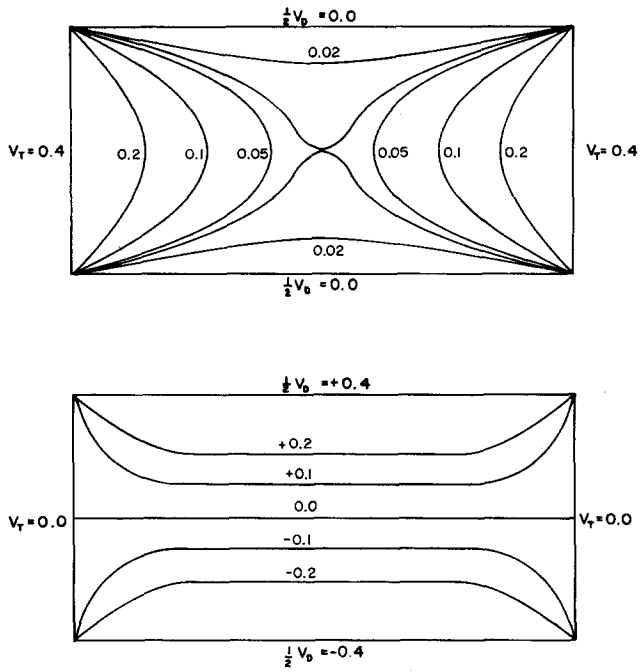

FIG. 1. Equipotentials obtained from an exact solution to Laplace's equation for separately applied trapping and drift voltages. The view shown represents a cross section in the x–z plane.

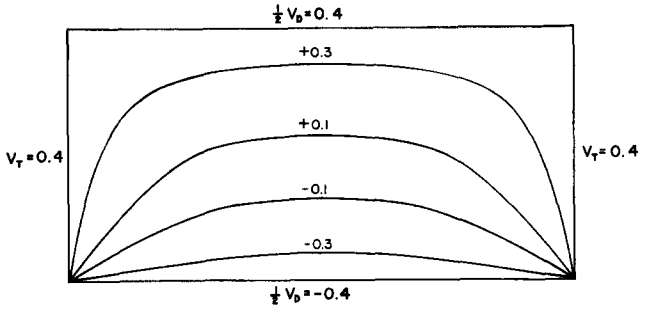

FIG. 2. Equipotentials for a typical experimental combination of trapping and drift voltages. Note that the trapping and drift characteristics are maintained in the combined fields.

II. ION MOTION IN THE ICR CELL

The trajectory of a particle of charge q and mass m subject to the combined action of an electric field $\mathbf{E}$ and magnetic field $\mathbf{H}$ can be determined from the solution of Eq. (4),

$$m\frac{d\mathbf{v}}{dt}=q\{\mathbf{E}+[(\mathbf{v}\times\mathbf{H})/c]\}. \tag{4}$$

In the absence of an applied electric field, the ion moves in a circular orbit in the plane perpendicular to $\mathbf{H}$ at the cyclotron frequency, $\omega_c=qH/mc$. Addition of a constant electric field gives rise to a net drift motion given by

$$\mathbf{v}_D=(c\mathbf{E}\times\mathbf{H})/H^2, \tag{5}$$

which will be in a direction perpendicular to both $\mathbf{E}$ and $\mathbf{H}$. In executing this drift motion, the center of the ion orbit *will remain on an equipotential* of the applied electric field

Combining the potentials given by Eqs. (2) and (3) gives

$$\mathbf{E}=-\nabla V=\left(\frac{3.52xV_T}{d^2}-\frac{2V_D}{d}\right)\mathbf{i}-\frac{7.04z}{d^2}\mathbf{k} \tag{6}$$

from which we have

$$\mathbf{v}_D=\left(\frac{3.52xV_T}{d^2}-\frac{2V_D}{d}\right)\frac{c}{H}\mathbf{j}. \tag{7}$$

In the more normal experimental situation, different voltages are applied to the source and resonance regions of the ICR cell. If we let V_{DS} and V_{DR} be the drift voltages in each region, respectively, then the corresponding drift velocities are

$$v_{DS}=(2cV_{DS}/Hd)-[(3.52xcV_T)/Hd^2] \tag{8}$$

and

$$v_{DR}=(2cV_{DR}/Hd)-[(3.52xcV_T)/Hd^2)] \tag{9}$$

in the negative y direction. If l_1 and l_2 are the distances from the electron beam to the beginning and end of the resonance region, respectively, then

$$\tau=l_1/v_{DS} \tag{10}$$

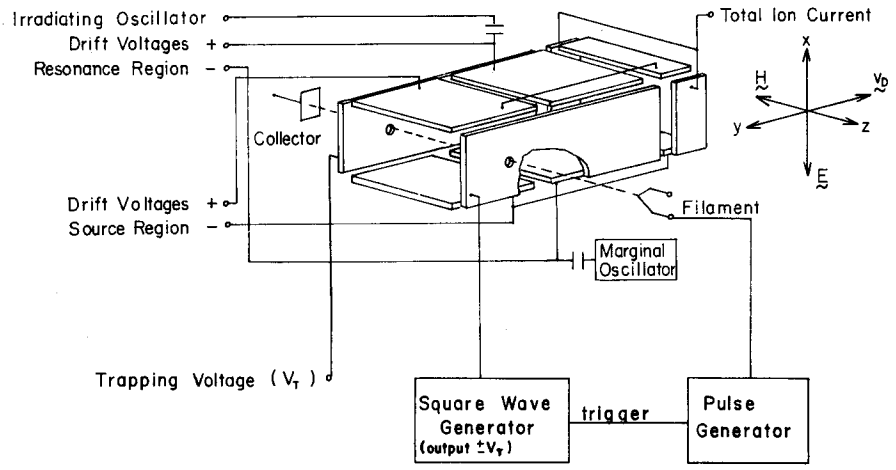

FIG. 3. Cutaway view of the ICR cell including a block diagram showing the modifications required to perform transit time experiments; trapping voltage is + for positive, − for negative ions.

and

$$\tau' = (l_1/v_{DS}) + [(l_2 - l_1)/v_{DR}]. \quad (11)$$

It should be noted that the drift velocity is predicted to be independent of trapping voltage only if the ions remain in the center of the cell in the plane defined by $x=0$. This is accomplished by balancing the drift voltages applied to the source and resonance regions so as to match the equipotentials in the center of the cell at the interface between the two regions. If the equipotentials are mismatched the ions will move out of the $x=0$ plane as they enter the resonance region.

III. DETERMINATION OF TRANSIT TIMES

A. Experimental Method

The ion cyclotron resonance spectrometer employed in this study is a V-5900 series manufactured by Varian Associates.[11] Modifications required to perform the ion transit time experiments are shown in Fig. 3. A Hewlett–Packard HP-3300 function generator generates a square wave of variable frequency and amplitude which is applied to one trapping plate of the ICR cell. The opposite trapping plate is held at a fixed potential equal to the square wave maximum voltage. The positive slope of the square wave is used to trigger a Tektronix type 161 pulse generator, providing a negative pulse of variable duration and magnitude which is applied to the filament to generate ions by switching the electron energy above the ionization threshold. In the present experiment the trapping plate was pulsed between ±0.40 V for times in the millisecond region corresponding to the ion transit times. The electron energy was pulsed from 10 to 43 eV for a duration of approximately 50 μsec. The trapping time is determined by the positive half-cycle of the square wave, measured directly to ±1.0 μsec with a Heath universal digital instrument model EU-805. The pulse sequence is illustrated in Fig. 4. The pulse times represent the on period of the square wave, which is equal to one-half the repetition rate period. Determination of transit times follows in a straightforward manner. An ion current is registered only if the trapping voltage remains on long enough for ions to reach the monitor. This technique is the simplest method for determining transit times. Difficulties are encountered in measuring the dispersion in arrival times since the ion current decreases inversely with trapping pulse width when the ion transit time is exceeded. To measure dis-

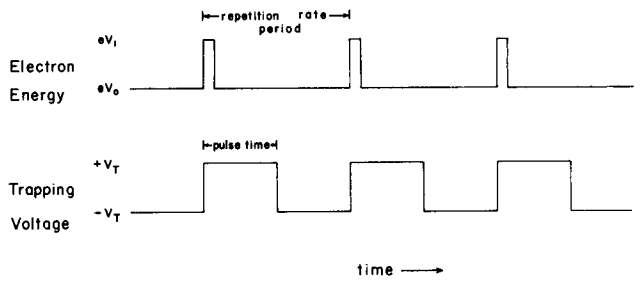

FIG. 4. Pulse sequence for transit time measurements. The electron energy is switched from below the ionization threshold (eV_0) to above (eV_1) to generate a pulse of ions. The pulse time defines the time during which ions are trapped in the cell. An ion current is registered if this exceeds the drift time through the cell.

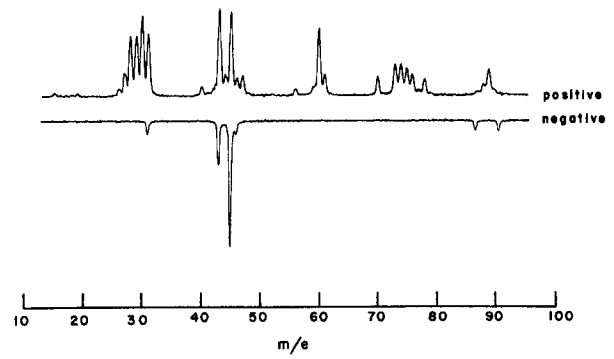

FIG. 5. Positive and negative ion cyclotron resonance spectra of a mixture of ethylnitrite (CH_3CH_2ONO) and ethanol (CH_3CH_2OH) recorded using trapping voltage modulation. Both spectra were recorded using the same gain and an observing oscillator frequency of 153.7 kHz; 25 eV, 10^{-5} Torr.

persion in arrival times, an alternate pulsing scheme was devised in which the repetition rate period, determined by the square wave generator, remains fixed at a period longer than the transit time. One of the trapping plates is held at a constant positive potential and the other is switched from this potential to a negative value after a suitable delay time, using a Tektronix type 161 pulse generator. Only if the delay period exceeds the transit time is an ion current registered. Referring to Fig. 4, this pulse sequence involves operation at a fixed repetition rate with a variable pulse time.

It is useful to note that it is possible to record ICR single resonance spectra by trapping voltage modulation. A single resonance spectrum is obtained in the absorption mode if one trapping plate is pulsed between some positive and negative potential with a period considerably longer than the ion transit time. A typical spectrum taken with trapping voltage modulation (25 Hz) is shown in Fig. 5 for a mixture of ethyl nitrite and ethanol. A simple reversal of the sign of the potential applied to the trapping plate held at constant voltage serves to trap negative rather than positive ions. The negative ion spectrum obtained under the same conditions as the positive ion spectrum is, as expected, 180° out of phase with the positive ion spectrum. Since mass discrimination effects are not important in ICR studies and the applied fields are inherently symmetrical for both positive and negative ions, it is possible to assess quantitatively the relative abundance of positive and negative ions. In addition, trapping voltage modulation is useful in the study of any phenomenon, such as photoionization or β decay, which generates ions over a large volume.

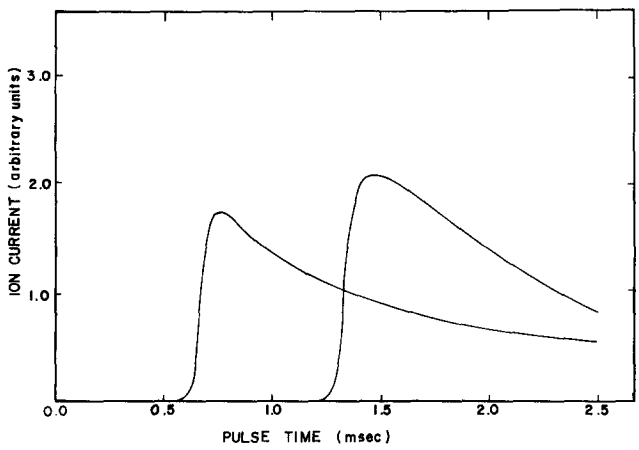

FIG. 6. Variation of ion current (N_2^+) with duration of pulse applied to the trapping plates, using the simpler pulsing method described in the text. Magnetic field strengths of 2.5 and 5.0 kG were employed, the latter corresponding to the longer transit time. Other conditions were $V_{DR}=V_{DS}=V_T=0.4$ V. Maximum ion currents of 10^{-11} A were recorded.

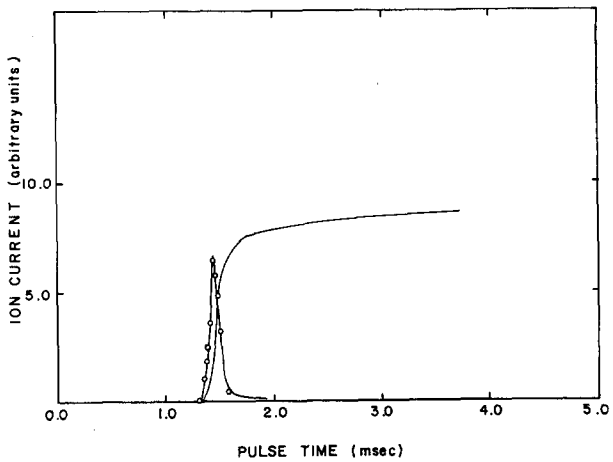

FIG. 7. Variation of ion current (N_2^+) with duration of pulse applied to the trapping plates using a fixed duty cycle for ion formation. The derivative of the ion current with respect to pulse time was determined by fitting a polynomial to the experimental curve at the indicated points. The derivative curve details the dispersion in transit times. Other conditions were the same as Fig. 6 with $H=5.0$ kG.

B. Variation of Transit Time with Magnetic Field Strength

The variation of ion current with pulse time using the simpler pulsed trapping method is illustrated in Fig. 6 for N_2^+ at a pressure of approximately 10^{-5} Torr and magnetic fields at 2.5 and 5.0 kG. The time at which the first ions arrive at the monitor was taken to be that time for which an ion current is first detectable. The maximum ion current gives the time at which the last ions formed in the electron beam pulse arrive at the electrometer. The mean arrival time of the ions is taken as that time at which the ion current attains one-half its maximum value. Assuming ion velocities in the range of 10^4–10^5 cm/sec we estimate that after they leave the resonance region it requires approximately 10–40 μsec for the ions to move to the side plates of the cell in the collector region (in which no trapping

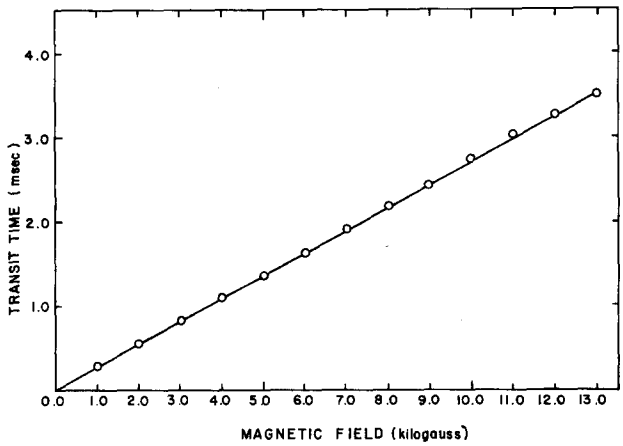

FIG. 8. Variation of ion transit time with magnetic field strength. The points represent experimentally determined mean ion transit times. The line indicates the calculated times using Eq. (11) in the text. Other conditions were $V_{DR}=V_{DS}=V_T=0.4$ V.

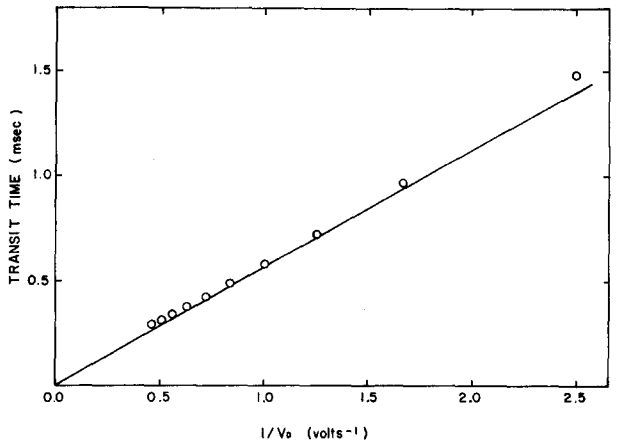

FIG. 9. Variation of ion transit time with drift voltage. The points represent experimentally determined mean ion transit times. The line indicates the calculated transit times using Eq. (11) in the text. Other conditions were $V_{DR}=V_{DS}=V_D$ (varied), $V_T=0.4$ V, $H=5.0$ kG.

voltage is applied). This error in transit time measurement is approximately canceled by the 50 μsec delay in formation of ions at the electron beam, following the turning on of the trapping.

The variation of ion current with trapping pulse time for the second pulsing scheme described above exhibits the expected step function behavior as shown in Fig. 7. The dispersion in ion transit times can be determined from the derivative of this curve, obtained by numerical analysis. The observed dispersion in transit times is small (about 100 μsec) as determined by the full width at half-height of the derivative curve displayed in Fig. 7. The spread in ion production and collection times contributes to this measured dispersion.

In Fig. 8 the experimental variation of ion transit time with magnetic field strength is compared with that calculated from Eq. (11) for ions at the center of the cell ($x=0$). The agreement is excellent for the range of magnetic fields available with our instrument (0–14 kG).

C. Variation of Transit Time with Drift Voltages

The variation of ion transit times with simultaneous variation of the drift voltages in the source and resonance regions is shown in Fig. 9. The line represents calculated transit times. As is evident, agreement is good for the full range of electric field strengths.

A simple transposition of Eqs. (10) and (11) gives

$$\tau'=\tau+[(l_2-l_1)Hd/2cV_{DR}]. \quad (12)$$

Thus by measuring the ion transit time at fixed magnetic field strength for various values of the drift voltage in the resonance region, V_{DR}, and making a plot of τ' vs V_{DR}^{-1}, the source residence time τ is obtained as the intercept of the τ' axis. Typical experimental results are shown in Fig. 10. The experimental value of τ is 0.39 msec, to be compared with a calculated source transit time of 0.41 msec. Relatively more weight is given to those points at higher values of V_{DR}^{-1}. Fringing of the electric fields in the source regions is likely to occur at high electric field strength in the resonance region and may cause the observed deviation from linearity at low values of V_{DR}^{-1} in Fig. 10.

D. Variation of Transit Time with Trapping Voltage

The effects of trapping voltage V_T and position of an ion in the cell, x/d, on the transit time of an ion are illustrated in Fig. 11. The results indicate a good qualitative agreement between experimental transit times and those calculated using ion velocities given by Eqs. (8) and (9). A lack of better quantitative agreement can be attributed to the approximation inherent in the parameterization of the electrostatic field in Eq. (11), which does not satisfy Laplace's equation ($\nabla^2V=0$) unless $A=B$. If the drift voltages are *balanced* in the source and resonance regions it is found, as predicted, that transit times are relatively insensitive to a wide range of trapping voltage.

E. Effects of Ion Energy on Transit Time

It is assumed in a double resonance experiment that at low irradiating power the change in product ion intensity observed upon irradiation of a reactant ion reflects the change in reaction rate with ion kinetic energy.[13] If the higher ion kinetic energy resulting from irradiation leads to a modification of the ion transit time, then the extent of conversion from reactant to product will be similarly altered, independent of any variation in the reaction rate constant with ion kinetic energy. To test this possibility the mean arrival times of ions were measured as a function of the field strength of the double resonance oscillator used to irradiate the only species present (N_2^+) in the source

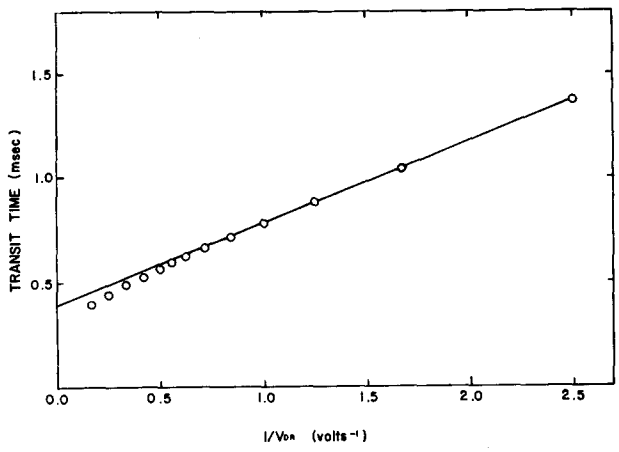

FIG. 10. Variation of transit time with drift voltage applied to the resonance region. Relatively more weight is given to the points at higher values of V_{DR}^{-1} to compensate for the effect of fringing fields. The transit time axis intercept is the source residence time. Other conditions were $V_{DS}=V_T=0.4$ V and $H=5.0$ kG.

region. Ion transit times were found to be independent of irradiating field strength up to the point where ions were ejected from the cell by striking the drift plates. This corresponds to an ion energy of ~100 eV.

F. Variation of Ion Transit Time with Pressure

At pressures high enough that a significant number of collisions occur in the ICR cell, it is necessary to consider possible effects this might have on the ion transit times. A damping term representing the effects of momentum transfer is added to Eq. (4) to give

$$m(d\mathbf{v}/dt)=q\{\mathbf{E}+[(\mathbf{v}\times\mathbf{H})/c]\}-\xi\mathbf{v}, \tag{13}$$

where ξ is the collision frequency for momentum transfer. The time averaged solution to this equation yields[14]

$$\langle v_x\rangle=\frac{\xi qE}{m(\omega_c^2+\xi^2)}\simeq\frac{\xi cE}{\omega_c H} \tag{14}$$

$$\langle v_y\rangle=\frac{-\omega_c qE}{m(\omega_c^2+\xi^2)}\simeq-\frac{cE}{H}\left[1-\left(\frac{\xi}{\omega_c}\right)^2\right]. \tag{15}$$

In the limit of no collisions $\langle v_x\rangle$ is zero and $\langle v_y\rangle$ gives the drift velocity. Based on the long range attraction between the ion–neutral pair being dominated by the ion-induced dipole interaction, the approximate collision frequency is given by[15–17]

$$\xi=2.21n\pi q\alpha^{\frac{1}{2}}\mu^{\frac{1}{2}}/m, \tag{16}$$

where n is the number density of neutrals, α is the angle averaged polarizability, and μ is the reduced mass of the collision pair.

Ion transit times were measured for N_2^+ at pressures up to 6×10^{-3} Torr with a magnetic field strength of 5.0 kG. At 6×10^{-3} Torr a collision frequency of 9.7×10^4 sec^{-1} is calculated from Eq. (16), while ω_c is 1.7×10^6 sec^{-1}. From Eq. (15) less than 1% decrease in transit time is predicted. This was experimentally verified within our limit of accuracy. No change in ion transit time was observed with increasing pressure, up to the highest pressure obtainable (6×10^{-3} Torr). At higher pressures, where the effect would measurably influence drift times, the loss of ions to the negative drift plate becomes appreciable in accordance with the pressure dependent transverse drift velocity given by Eq. (14). A measurable ion current is, however, not registered under such conditions, and transit times cannot be determined.

IV. DISCUSSION

It is evident that measured transit times are adequately reproduced by the straightforward analysis leading to Eqs. (10) and (11) when the drift voltages applied to the source and resonance regions are appropriately balanced so as to match, at the center of the cell, the equipotential

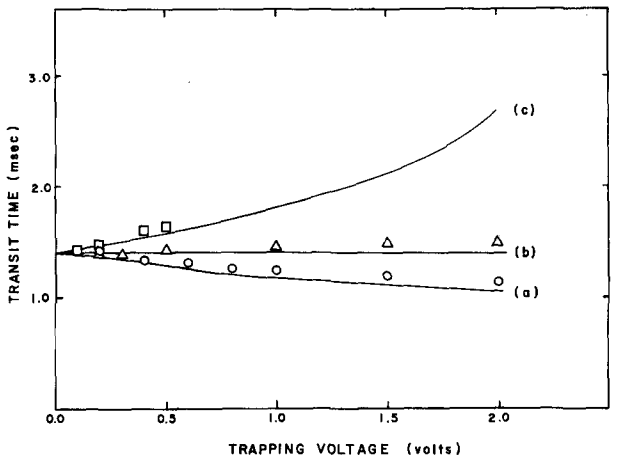

FIG. 11. Effect of trapping voltage on ion transit time for three different field situations: (a) $V_{DR}=0.4$ V (+0.3 V on top plate and −0.1 V on bottom plate). (b) $V_{DR}=0.4$ V (+0.2 V on top plate and −0.2 V on bottom plate). (c) $V_{DR}=0.4$ V (+0.1 V on top plate and −0.3 V on bottom plate). In each case $V_T=V_{DS}=0.4$ V with the drift voltage divided evenly between the top and bottom plates in the source region. Other conditions were $H=5.0$ kG. In the three cases shown the ions are in the plane defined by (a) $x=+d/4$, (b) $x=0$, and (c) $x=-d/4$ as they pass through the resonance region.

along which the ions move in each region. The trapping voltage is found to influence transit times *only* when the drift equipotentials are mismatched at the center of the cell. It is essential to periodically subject the cell to extensive cleaning in trichlorotrifluoroethane using an ultrasonic bath followed by high temperature bakeout (200°C) in vacuum. This minimizes the deleterious effects of surface potentials which would easily become important relative to the rather low applied voltages. In this respect, surface charging is minimized by maintaining, where feasible, a low impedance to ground in all electrical connections to the plates of the ICR cell. Even when surface potentials cause deviations from expected behavior, the technique described for directly measuring transit times can be employed to reproducibly and accurately determine reaction rate constants. A cell in which the spacing between the drift electrodes is further reduced would provide greater homogeneity from the drift field. In such a cell, however, resonant ions striking the drift electrodes would likely become a serious problem. The experiments described herein suggest that the present cell design provides adequate control of the ion motion for meaningful kinetic measurements.

Although the present experiments describe transit time measurements with a nonreactive system, we have obtained equally good results with a variety of complex organic molecules.

ACKNOWLEDGMENTS

We are indebted to P. G. Miasek for his assistance in analyzing the electrostatic fields in the cyclotron resonance

cell. One of us (TBM) wishes to thank the National Research Council of Canada for fellowship support. This work was supported by the United States Atomic Energy Commission under Grant AT(04-3)767-8.

* Alfred P. Sloan fellow, 1968–1970.
† Contribution No. 4189.
[1] J. D. Baldeschwieler, Science **159**, 263 (1968).
[2] L. R. Anders, J. L. Beauchamp, R. C. Dunbar, and J. D. Baldeschwieler, J. Chem. Phys. **45**, 1062 (1966).
[3] J. L. Beauchamp, L. R. Anders, and J. D. Baldeschwieler, J. Amer. Chem. Soc. **89**, 4569 (1967).
[4] J. L. Beauchamp and R. C. Dunbar, J. Amer. Chem. Soc. **92**, 1477 (1970).
[5] J. L. Beauchamp and J. T. Armstrong, Rev. Sci. Instrum. **40**, 123 (1969).
[6] D. Holtz, J. L. Beauchamp, and J. R. Eyler, J. Amer. Chem. Soc. **92**, 7045 (1970).
[7] L. R. Anders, J. Phys. Chem. **73**, 469 (1969).
[8] R. P. Clow and J. H. Futrell, Int. J. Mass Spectrosc. Ion Phys. **4**, 165 (1970).
[9] S. E. Buttrill, Jr., J. Chem. Phys. **50**, 4125 (1969).
[10] A. G. Marshall and S. E. Buttrill, Jr., J. Chem. Phys. **52**, 2752 (1970).
[11] M. B. Comisarow, J. Chem. Phys. **55**, 205 (1971).
[12] V-5900 ICR mass spectrometer, Varian Associates.
[13] J. L. Beauchamp and S. E. Buttrill, Jr., J. Chem. Phys. **48**, 1783 (1968).
[14] J. L. Beauchamp, Ph.D. thesis, Harvard University, 1967.
[15] J. L. Beauchamp, J. Chem. Phys. **46**, 1231 (1967).
[16] E. W. McDaniel, *Collision Phenomena in Ionized Gases* (Wiley, New York, 1964).
[17] It should be noted that collision frequencies calculated for N_2^+ in N_2 with Eq. (16) will be somewhat low due to the occurrence of charge exchange outside the orbiting impact parameter.

THE REVIEW OF SCIENTIFIC INSTRUMENTS VOLUME 42, NUMBER 11 NOVEMBER 1971

High Stability Electrodeless Discharge Lamps*

WILLIAM S. GLEASON
Shell Development Company, Emeryville, California 94608
AND
RICHARD PERTEL
Institute of Gas Technology, IIT Center, Chicago, Illinois 60616

(Received 6 July 1971)

A detailed procedure is described for the laboratory construction of electrodeless discharge lamps. Although this work pertains to Hg in Ar discharges, the same general experimental techniques are also applicable for other substances. The lamps made were without any getters and had an intensity variation of less than one part in 1000 over a period of 50 h of continuous operation. The described procedure allows for continuous monitoring of critical cleaning procedures in the evacuated lamp blank before it is filled and sealed off.

INTRODUCTION

In recent years the electrodeless discharge lamp has found increasingly wider application in the fields of spectroscopy,[1–6] photochemistry,[7–14] and analytical chemistry.[15–17] Since it is used as a low pressure lamp in most cases, such discharges provide a relatively high intensity of resonance radiation frequencies of the substance being excited. It is also possible to operate these lamps under conditions where self-reversal and line broadening are strongly minimized. The Doppler half-widths of the atomic resonance lines are typically about 20–150 mK and are for a given line proportional to $(T/M)^{\frac{1}{2}}$, where T is the temperature of the system in degrees Kelvin and M is the atomic weight of the emitter. Thus it is possible to excite individual hyperfine structure components for photochemical[7–9] as well as spectroscopic applications.[2,18,19] The lamp is excited by a microwave field, usually at 2450 MHz owing to the ready commercial availability of suitable generators. Because electrode sputtering and chemical interaction of plasma with the electrodes are absent, electrodeless discharges have found wide use when small samples of high purity have to be excited, e.g., isotopically pure samples.

The loss of light intensity due to "clean-up" can be easily restored by a gentle heating of the lamp. Finally, the lamp consists of nothing more than a small sealed tube containing a few milligrams of the sample and some inert gas such as argon as a sensitizer. This simple construction makes it possible to produce the lamp in the laboratory.

One of the main disadvantages of this type of lamp has been the tendency to flicker due to the instability in the plasma caused by impurities introduced during construction. This problem can be partially resolved by the addition of a getter. However, this introduces an additional source of contamination.

Our studies of the quenching cross section values for various gases with excited mercury required the construction of a high intensity electrodeless discharge lamp containing isotopic mercury without a getter which had intensity fluctuations of less than one part per 1000 during continuous operation over a period of 50 h. Although the procedure which was developed was applied to the con-